structurally characterized macrocyclic compound having the $-CH{=}N(CH_2)_4N{=}CH-$ group. That $[Cu(cis\text{-}[18]diene\text{-}N_4)](ClO_4)_2$ exhibits a tetrahedral distortion nearly twice as large as that of **3** may be attributed to the interaction between methylene hydrogens on C(1) and C(4) in the tetramethylene bridge and methyl hydrogens on C(6) and C(20). The second tetramethylene bridge (not present in **3**) may also contribute to the tetrahedral distortion. A small tetrahedral distortion has also been observed in 6,8,8,13,13,15-hexamethyl-1,2,4,5,9,12-hexaazacyclopentadec-5,14-diene-3-spirocyclohexane,[31] but the details of this structure have not yet been reported. The distortion in this complex is apparently due to the presence of the spirocyclohexane group.

The less distorted geometry of the trans complex is more favorable for coordination of copper(II), as illustrated by the greater yield of the red trans complex during the template condensation. Once the compounds are formed, however, the distorted geometry of the cis complex appears to protect it to some extent from hydrolysis at the double bond. Hydrolysis of these bonds in the trans complex can be assisted by coordination of water to copper(II) above and below the plane of the macrocycle, where they have easy access to the double bonds. Coordination of water to copper(II) in the cis complex is sterically inhibited.

Tetrahedrally distorted complexes of Cu(II) have been of interest as models for copper proteins such as the blue copper proteins.[32-34] In the cis compound reported here, the reduction of copper(II) to copper(I) should be aided by the tetrahedral distortion in the copper(II) complex. By analogy to the geometry in the macrocyclic complex (1,1-difluoro-4,5,11,12-tetramethyl-1-bora-3,6,10,13-tetraaza-2,14-dioxacyclotetradeca-3,5,10,12-tetraenato)copper(I),[35] which is intermediate between tetrahedral and square planar, it is likely that the geometry in Cu(I) complexes of the macrocycles described here will be distorted toward square-planar configurations. Furthermore, the combination of two imine and two amine donors should not heavily favor either oxidation state of copper. This situation is ideal for modeling oxidases, which must cycle between copper(II) and copper(I). The redox reaction of such enzymes is made more favorable by means of coordination goemetries which favor neither oxidation state but rather adopt intermediate geometries. The cis macrocyclic complex shows promise of providing intermediate geometries similar to those observed in the enzymes.

Macrocyclic complexes have additional promise as copper oxidase models because large variations in chelate ring size, double-bond placement, and side chains may be achieved by straightforward synthetic methods involving only a few steps. Oxidation and reduction of the ligands can provide further variation. By these methods it should be possible to tailor ligands to achieve tetrahedral distortions of varying magnitude for use in model studies. Further investigations of this nature are presently being undertaken in this laboratory.

Acknowledgment. This work was supported by Grant No. A-259 from The Robert A. Welch Foundation.

Registry No. I, 73429-78-4; II, 72765-21-0.

Supplementary Material Available: Tables of observed and calculated structure factors (15 pages). Ordering information is given on any current masthead page.

(30) Losman, D.; Englehard, L. M.; Green, M. *Inorg. Nucl. Chem. Lett.* **1973**, *9*, 791.
(31) Curtis, N. F. In "Coordination Chemistry of Macrocyclic Compounds"; Melson, G. A., Ed.; Plenum: New York, 1979; p 300.
(32) Osterburg, R. *Coord. Chem. Rev.* **1974**, *12*, 309.
(33) Patterson, G. S.; Holm, R. H. *Bioinorg. Chem.* **1975**, *4*, 257.
(34) Malkin, R. *Inorg. Biochem.* **1973**, *3*, 689.
(35) Gagné, R. R.; Allison, J. L.; Lisensky, G. C. *Inorg. Chem.* **1978**, *17*, 3563.
(36) Johnson, C. K. Report ORNL-3794; Oak Ridge National Laboratory: Oak Ridge, Tenn., 1965.

Contribution from the Department of Chemistry, State University of New York at Stony Brook, Stony Brook, New York 11794

Synthesis and Molecular Structure of $(\eta^3\text{-}C_3H_5)Fe(CO)_3AuP(C_6H_5)_3$ and the Molecular Structure of $(\eta^3\text{-}C_3H_5)Fe(CO)_3Br$. Two Compounds with Distinctly Different Coordination Geometries

FREDERICK E. SIMON and JOSEPH W. LAUHER*

Received October 29, 1979

The compound $(\eta^3\text{-}C_3H_5)Fe(CO)_3AuP(C_6H_5)_3$ has been synthesized and its molecular structure solved by X-ray diffraction techniques, space group $C2/c$ with $a = 30.76$ (2) Å, $b = 11.60$ (1) Å, $c = 13.54$ (2) Å, $\beta = 110.38$ (1)°, and $Z = 8$. The molecular structure of $(\eta^3\text{-}C_3H_5)Fe(CO)_3Br$ was also determined, space group *Pnma* with $a = 11.497$ (7) Å, $b = 7.962$ (4) Å, $c = 9.556$ (4) Å, and $Z = 4$. The coordination geometries of the two compounds are distinctly different. The bromide derivative has a conventional pseudooctahedral geometry while the gold derivative has an unusual geometry which may be described best as a trigonal-bipyramidal $(\eta^3\text{-}C_3H_5Fe)(CO)_3$ moiety with a $AuP(C_6H_5)_3$ ligand located on an edge between two equatorial CO ligands. The resulting Au-Fe-CO angles are acute 70.9 (2) and 72.0 (2)°. The unusual structure may be due to the reversed polarity of the iron-gold bond as compared to the iron-bromide bond. Spectral evidence suggests that there is a high negative charge on the iron atom of the gold derivative.

Introduction

The η^3-allyliron tricarbonyl halides and pseudohalides are known to exist in two conformational isomers in solution. The geometry of each isomer is approximately octahedral with the allyl ligand occupying two cis positions. In the endo isomer, **1**, the allyl points away from the halide, while in the exo isomer, **2**, it points toward the halide.

The existence of the two isomers was first hypothesized by Nesmeyanov and co-workers[1] and was confirmed by Faller and

(1) Nesmeyanov, A. N.; Ustynyuk, Yu. A.; Kritskaya, I. I.; Shchembelov, G. A. *J. Organomet. Chem.* **1968**, *14*, 395.

0020-1669/80/1319-2338$01.00/0

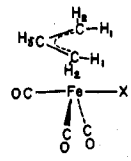

endo

1

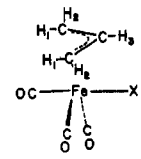

exo

2

Adams[2] who determined that the predominate isomer in solution has the endo configuration. The crystal structure of the iodide derivative has been reported[3] and it also consists of the endo isomer. The structure of the dinuclear complex $[(\eta^3\text{-}C_3H_5)Fe(CO)_3]_2$,[4] **3**, has been shown to consist of two exo radical monomers coupled together with a long Fe–Fe bond, 3.138 (3) Å.

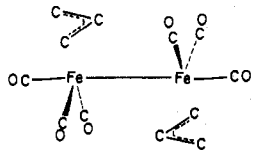

3

We wish to report the synthesis and characterization of a new member of the $(\eta^3\text{-}C_3H_5)Fe(CO)_3X$ series in which the fifth substituent is a (triphenylphosphine)gold(I) cation. The molecular structure of this new compound has been determined and has proven to be most unusual. For comparison purposes, we examined the structure of the bromide, $(\eta^3\text{-}C_3H_5)Fe(CO)_3Br$, which has the endo geometry in the crystalline state.

Experimental Section

All solvents were dried by standard procedures and distilled under a dinitrogen atmosphere before use. Reactions were carried out in a Vacuum Atmospheres Corp. glovebox under a dry, N_2 atmosphere. $(\eta^3\text{-}C_3H_5)Fe(CO)_3Br$[4] and $(1\text{-}C_6H_5\text{-}\eta^3\text{-}C_3H_4)Fe(CO)_3Br$[5] were prepared by literature methods and recrystallized before use. $AuPPh_3Cl$ was made by the method of Ingold and Gregory.[6] Infrared spectra were recorded with a Perkin-Elmer 567 spectrometer using a CsBr solution cell or KBr for the solid-state spectra. ^1H NMR spectra were recorded on a Varian EM-360 60-MHz NMR spectrometer or a Varian HFT-80 for the low-temperature studies, using Me_4Si as an internal standard.

Preparation of $(\eta^3\text{-}C_3H_5)Fe(CO)_3AuP(C_6H_5)_3$. A reaction slurry of 1.0 g (3.8 mmol) of $(\eta^3\text{-}C_3H_5)Fe(CO)_3Br$ and 0.7 g of zinc dust in 70 mL of diethyl ether was stirred for 2 h at room temperature. The solution turned deep red and then yellow over the reaction period. Excess zinc was removed by filtration and $AuPPh_3Cl$ (1.9 g, 3.18 mmol) was added. The slurry was allowed to react for 6 h at room temperature. The grayish mixture was then filtered through a glass frit to give a clear, yellow solution, and the ether was removed under vacuum. A 150-mL sample of hexane was added in 50-mL portions with vigorous shaking to extract the product. The combined extracts were reduced in volume to about 50 mL and allowed to set overnight at −40 °C to yield small, yellow crystals. These were collected and dried in vacuo: yield 1.0 g (43%); mp 100–110 °C dec. Infrared data are listed in Table I and NMR data in Table II.

Table I. Infrared Data for Compounds $(\eta^3\text{-}C_3H_5)Fe(CO)_3X$[a]

X	ν_1	ν_2	ν_3
NO_2	2062	2053	2108
NO_3	2021	2064	2108
CF_3COO	2011	2055	2101
Cl	2012	2050	2097
Br	2011	2045	2091
I	2010	2032	2080
$(\eta^3\text{-}C_3H_5)Fe(CO)_3$	1960	1968	2046
	1890	1915	1987
$(C_6H_5)_3PAu$	1903[b]	1930	1993
	1880[c]	1910	1985

[a] Carbonyl stretching frequencies (cm^{-1}) in $CHCl_3$.[7] [b] In hexane. [c] In Nujol (mull).

Preparation of $(1\text{-}C_6H_5\text{-}\eta^3\text{-}C_3H_4)Fe(CO)_3AuP(C_6H_5)_3$. A 1.0-g sample of $(1\text{-}C_6H_5\text{-}\eta^3\text{-}C_3H_4)Fe(CO)_3Br$ and 1.0 g of 200-mesh magnesium metal in 100 mL of THF were allowed to react while being stirred vigorously for 4 h. A color change from dark brown to red indicated that a reaction was occurring. The slurry was then filtered to remove excess Mg, and the THF was removed under vacuum, 100 mL of diethyl ether and 1.5 g of $AuPPh_3Cl$ were added, and the mixture was stirred for 6 h. The reaction mixture was filtered to give a clear, yellow solution which was reduced to about 10 mL and chromatographed on neutral alumina using 1:1 ether–hexane (v/v). Collection of the yellow band and crystallization from pentane yielded 0.1 g (6%) of product.

X-ray Diffraction Studies. Data were collected for both $(\eta^3\text{-}C_3H_5)Fe(CO)_3AuP(C_6H_5)_3$ and $(\eta^3\text{-}C_3H_5)Fe(CO)_3Br$ on an Enraf-Nonius CAD-4A automated diffractometer under the control of a PDP 11/45 computing system using Mo Kα radiation. Three standard reflections were measured every 100 reflections to assess crystal movement or decomposition. The standards for the bromide were found to decay about 20%, while for the gold derivative there was no significant deviation. The data were reduced ($p = 0.04$) and corrected for intensity decay, and a numerical absorption correction was applied.[8]

For $(\eta^3\text{-}C_3H_5)Fe(CO)_3Br$ (Table III), a Patterson synthesis revealed the location of the bromide atom on the mirror plane. A subsequent difference Fourier located the other nonhydrogen atoms. After anisotropic refinement of the heavy atoms, a difference Fourier map clearly revealed the location of all the hydrogen atoms. They were assigned isotropic temperature factors of 5.0 Å^2 and added as a fixed contribution for the remainder of the refinement. The function minimized in the least squares was $\sum w(|F_o| - |F_c|)^2$, $R = \sum[|F_o| - |F_c|]/\sum|F_o|$, $R_w = [\sum w(|F_o| - |F_c|)^2/\sum wF_o^2]^{1/2}$, $w = 1/(\sigma^2 + 0.0016F_o^2)$. Anomalous dispersion corrections were made for all nonhydrogen atoms. Final positional and thermal parameters are given in Table IV and the derived bond distances and angles in Table VI.

For $(\eta^3\text{-}C_3H_5)Fe(CO)_3AuP(C_6H_5)_3$ (Table III), the gold atom was easily located from the Patterson map, and the other nonhydrogen atoms were located through several cycles of least-squares and difference Fourier synthesis. After refinement using anisotropic thermal parameters, the hydrogen positions were calculated assuming ideal geometries around the phenyl groups and the allyl ligand. They were assigned isotropic temperature factors of 6.0 Å^2 and added as a fixed contribution for the remainder of the refinement. Final positional and thermal parameters are given in Table V and the derived bond distances and angles in Table VII.

Results and Discussion

Syntheses and Spectra. The compound $(\eta^3\text{-}C_3H_5)Fe(CO)_3Br$, I, can be easily prepared by the direct reaction of allyl bromide with $Fe_2(CO)_9$ in hexane. The resulting bromide complex reacts with zinc dust in diethyl ether to give a yellow solution which contains what is probably a zinc complex of the $[(\eta^3\text{-}C_3H_5)Fe(CO)_3]^-$ anion. This solution reacts with $AuP(C_6H_5)_3Cl$ to give the desired $(\eta^3\text{-}C_3H_5)Fe(CO)_3AuP$-

(2) Faller, J. W.; Adams, M. A. *J. Organomet. Chem.* **1979**, *170*, 71.
(3) (a) Minasyants, M. K.; Struchkov, Yu. T.; Kritskaya, I. I.; Avoyan, R. L. *J. Struct. Chem. (Engl. Transl.)* **1966**, *7*, 840. (b) Chenskaya, T. B.; Lokshin, B. V.; Kritskaya, I. I. *Bull. Acad. Sci. USSR, Div. Chem. Sci. (Engl. Transl.)* **1973**, *22*, 1105.
(4) Putnik, C. F.; Welter, J. J.; Stucky, G. D.; D'Aniello, M. J.; Sosinsky, B. A.; Kirner, J. F.; Muetterties, E. L. *J. Am. Chem. Soc.* **1978**, *100*, 4107.
(5) Nesmeyanov, A. N.; Nekrasov, Y. S.; Avakyan, N. P.; Kritskaya, I. I. *J. Organomet. Chem.* **1971**, *33*, 375.
(6) Ingold, C. K.; Gregory, B. J. *J. Chem. Soc. B* **1969**, 276.
(7) Chenskaya, T. B.; Lokshin, B. V.; Kritskaya, I. I. *Bull. Acad. Sci. USSR, Div. Chem. Sci. (Engl. Transl.)* **1973**, *22*, 1105; except for $AuP(C_6H_5)_3$.
(8) The programs used were those of the Enraf-Nonius structure determination package.[9]
(9) Okaya, Y. In "Computing in Crystallography"; Schenk, H., Olthof-Hazekamp, R., van Koningsveld, H., Bassi, G. C., Eds.; Delft University Press: 1978; pp 153–165. Frenz, B. A. *Ibid.* pp 64–71.

Table II. NMR Chemical Shift Data for Some $(\eta^3\text{-}C_3H_5)Fe(CO)_3X$ Derivatives

X	solvent	NMR, δ H₁ endo	H₁ exo	H₂ endo	H₂ exo	H₃ endo	H₃ exo	$J(H_1\text{-}H_3)$, Hz	$J(H_2\text{-}H_3)$, Hz	isomer ratio endo:exo	ref
NO_3	$CDCl_3$	2.60		4.66		5.27		15	7.5		3b
NCO	$CDCl_3$	3.05	2.65	4.47	4.32	5.15	5.05			24:1	2
Cl	$CDCl_3$	3.17	2.59	4.44	4.18	5.07	5.80	14.7	7.7	7.7:1	3b
Br	$CDCl_3$	3.45	2.57	4.40	4.10	4.90		13.5	6.0	3:1	2
I	CCl_4	3.73	2.21	4.09	3.71	4.52	5.86	13.0	7.5	2.2:1	3b
$AuP(C_6H_5)_3$	$CDCl_3$	1.62		2.66				11.0	6.0		
	$(CD_3)_2CO$	1.62		2.67		4.85		10.6	6.2		

Table III. Crystal Data and Data Collection Procedures

	$(\eta^3\text{-}C_3H_5)Fe(CO)_3Br$	$(\eta^3\text{-}C_3H_5)Fe(CO)_3AuP(C_6H_5)_3$
formula	$C_6H_5O_3BrFe$	$C_{24}H_{20}O_3AuFeP$
mol wt	260.86	640.21
space group	*Pnma* (orthorhombic)	*C*2/*c* (monoclinic)
a, Å	11.497 (7)	30.76 (2)
b, Å	7.962 (4)	11.60 (1)
c, Å	9.556 (4)	13.54 (2)
β, deg		110.38 (1)
V, Å³	874.7	4530
Z	4	8
ρ(calcd), g/cm³	1.981	1.877
ρ(measd), g/cm³		1.86 (1)
cryst shape, mm	0.24 × 0.34 × 0.38	0.12 × 0.18 × 0.44
radiation	Mo Kα (λ = 0.710 73 Å) with a graphite monochromator	Mo Kα (λ = 0.710 73 Å) with a graphite monochromator
scan mode	ω–2θ	ω–2θ
2θ range, deg	0 < 2θ < 60	0 < 2θ < 52
reflctns	2003 collected, 489 unique with $\lvert F_o\rvert^2 > 3\sigma\lvert F_o\rvert^2$ used; 59 variables	5708 collected, 2813 unique with $\lvert F_o\rvert^2 > 3\sigma\lvert F_o\rvert^2$ used; 271 variables
linear abs coeff, cm⁻¹	65.64	74.34
transmission factors	min 5.99, max 24.75, av 20.84	min 12.36, max 56.29, av 37.86
error in obsrvn of unit weight, e	2.397	2.481
temp, °C	22	22
R	0.075	0.050
R_w	0.082	0.064

Table IV. Positional and Thermal Parameters and Their Estimated Standard Deviations for $(\eta^3\text{-}C_3H_5)Fe(CO)_3Br$[a]

atom	*x*	*y*	*z*	B_{11}	B_{22}	B_{33}	B_{12}	B_{13}	B_{23}
Br	0.2579 (2)	1/4	0.1612 (2)	10.6 (2)	6.4 (1)	3.8 (1)	0	0.3 (1)	0
Fe	0.2285 (2)	1/4	0.4198 (2)	4.2 (1)	4.0 (1)	3.8 (1)	0	−0.2 (1)	0
O(4)	0.4181 (8)	0.042 (1)	0.8568 (8)	9.4 (5)	6.3 (5)	7.4 (4)	−2.7 (4)	1.2 (4)	0.8 (4)
O(5)	0.1552 (11)	1/4	0.7117 (10)	7.9 (5)	7.3 (8)	4.4 (7)	0	0.8 (4)	0
C(1)	0.3786 (10)	0.095 (2)	0.439 (1)	7.0 (5)	5.9 (5)	6.0 (7)	2.0 (5)	0.8 (6)	1.0 (6)
C(2)	0.3933 (14)	1/4	0.504 (2)	4.7 (5)	6.9 (1)	6.1 (7)	0	−0.7 (6)	0
C(4)	0.1397 (9)	0.071 (1)	0.384 (1)	5.5 (5)	5.2 (5)	4.6 (4)	1.3 (5)	−1.2 (4)	−0.1 (6)
C(5)	0.1859 (14)	1/4	0.600 (2)	5.6 (5)	6.9 (1)	4.0 (7)	0	2.1 (6)	0

[a] The form of the anisotropic thermal parameter is $\exp[-1/4\{B_{11}(a^*h)^2 + B_{22}(b^*k)^2 + B_{33}(c^*l)^2 + 2B_{12}a^*b^*hk + 2B_{13}a^*c^*hl + 2B_{23}b^*c^*kl\}]$.

$(C_6H_5)_3$, II, in a reasonable (48%) yield. By use of cinnamyl bromide and $Fe_2(CO)_9$, the complex $(1\text{-}C_6H_5\text{-}\eta^3\text{-}C_3H_4)Fe(CO)_3Br$, III, can be prepared. The IR spectrum of III in pentane has peaks at 2090, 2060, and 2020 cm⁻¹ and the NMR spectrum ($CDCl_3$) shows peaks [1 H, δ 3.35 (d); 1 H, δ 4.22 (d); 1 H, δ 5.30 (m); 1 H, δ 5.56 (m)] for the allyl ligand as well as for the phenyl substituent [5 H, δ 7.2–7.5 (m)]. The reaction of III with zinc dust does not proceed in a satisfactory manner; however, III does react with magnesium metal in THF to produce a red solution. $AuP(C_6H_5)_3Cl$ was added to this solution to give $(1\text{-}C_6H_5\text{-}\eta^3\text{-}C_3H_4)Fe(CO)_3AuP(C_6H_5)_3$, IV, in poor yield (6%). The IR spectrum of IV in pentane has peaks at 2000, 1954, and 1900 cm⁻¹ which are lower in frequency than those of the corresponding bromide complex. The NMR spectrum (C_6D_6) is shifted upfield, analogous to the unsubstituted allyl complexes [1 H, δ 2.15 (d); 1 H, δ 3.50 (m); 1 H, δ 5.00 (m); 1 H, δ 6.30 (m); 5 H, δ 7.0–7.3 (m)]. However, no reliable interpretation of the NMR spectrum could be made due to the rapid formation of paramagnetic species in solution. The entire cinnamyl bromide reaction sequence is complicated by the formation of what we believe to be the neutral radical, $(1\text{-}C_6H_5\text{-}\eta^3\text{-}C_3H_4)Fe(CO)_3$. The phenyl substituent appears to stabilize that radical relative to the unsubstituted $(\eta^3\text{-}C_3H_5)Fe(CO)_3$ analogue.

The infrared data showing the carbonyl stretching frequencies for a variety of $(\eta^3\text{-}C_3H_5)Fe(CO)_3X$ derivatives are shown in Table I. The data show a direct correlation between the CO stretching frequencies and the donor ability of the substituent X. The highest frequencies are found for oxygen donor ligands such as NO_3^- with the halides following in the order of decreasing electronegativity. Intermediate values are found for the dimer, $[(\eta^3\text{-}C_3H_5)Fe(CO)_3]_2$, and the lowest values by far are exhibited by the gold complex, II. Assignments of formal oxidation states are always a matter of controversy, but we feel that the simple halide complexes may be regarded as normal Lewis base complexes of the Lewis acid $(\eta^3\text{-}C_3H_5)Fe(CO)_3^+$. On the other hand, the gold complex is best treated as a (triphenylphosphine)gold(I) Lewis acid ad-

Table V. Positional and Thermal Parameters and Their Estimated Standard Deviations for $(\eta^3\text{-}C_3H_5)Fe(CO)_3AuP(C_6H_5)_3$[a]

atom	x	y	z	B_{11}	B_{22}	B_{33}	B_{12}	B_{13}	B_{23}
Au	0.11924 (1)	0.15583 (3)	0.39702 (3)	4.81 (0)	2.35 (2)	4.49 (1)	0.36 (1)	1.92 (1)	−0.04 (1)
Fe	0.10346 (5)	0.3628 (1)	0.4296 (1)	4.84 (3)	2.06 (5)	5.54 (6)	−0.10 (4)	2.26 (4)	0.00 (6)
P	0.13296 (8)	0.9744 (2)	0.3514 (2)	3.83 (9)	2.43 (9)	4.36 (6)	0.37 (6)	1.51 (6)	0.0 (8)
O(4)	0.1343 (3)	0.3940 (9)	0.6564 (6)	7.7 (3)	6.8 (3)	6.1 (3)	−0.8 (3)	3.3 (2)	−0.8 (3)
O(5)	0.1990 (3)	0.3513 (9)	0.4360 (8)	6.6 (4)	8.8 (4)	9.0 (4)	−2.7 (3)	4.5 (2)	−1.4 (3)
O(6)	0.0174 (2)	0.2330 (8)	0.3919 (6)	5.2 (3)	5.4 (3)	7.7 (3)	−1.3 (3)	2.8 (2)	−0.9 (3)
C(1)	0.0766 (5)	0.4171 (12)	0.2695 (12)	9.4 (8)	4.0 (5)	8.9 (6)	−0.1 (5)	3.5 (6)	1.7 (6)
C(2)	0.0892 (7)	0.5048 (14)	0.3415 (15)	13.7 (10)	5.7 (6)	15.2 (9)	3.6 (6)	6.5 (7)	5.7 (6)
C(3)	0.0735 (6)	0.5306 (12)	0.4157 (15)	10.2 (10)	3.3 (4)	12.9 (9)	1.8 (5)	2.0 (8)	−0.1 (3)
C(4)	0.1215 (4)	0.3794 (10)	0.5682 (9)	5.4 (4)	3.6 (4)	5.4 (4)	−0.7 (3)	2.7 (3)	−0.5 (3)
C(5)	0.1614 (4)	0.3535 (9)	0.4322 (9)	6.4 (4)	3.8 (4)	6.3 (4)	−1.0 (3)	3.7 (3)	−0.3 (3)
C(6)	0.0520 (3)	0.2798 (9)	0.4090 (8)	4.8 (4)	3.0 (4)	5.6 (4)	0.1 (3)	2.3 (3)	0.3 (3)
C(11)	0.1776 (3)	0.9764 (9)	0.2929 (7)	4.2 (3)	3.4 (3)	3.2 (3)	0.7 (3)	1.2 (2)	0.4 (3)
C(12)	0.2134 (3)	0.0584 (11)	0.3307 (9)	4.1 (3)	4.9 (4)	6.0 (4)	−0.6 (4)	1.8 (3)	−0.1 (3)
C(13)	0.2473 (4)	0.0651 (12)	0.2863 (11)	4.2 (3)	5.8 (6)	8.6 (6)	−0.3 (4)	2.4 (4)	0.1 (6)
C(14)	0.2474 (4)	−0.0033 (11)	0.2077 (9)	5.6 (3)	6.0 (4)	5.7 (4)	1.6 (4)	2.3 (3)	0.5 (6)
C(15)	0.2112 (4)	0.9106 (11)	0.1659 (9)	5.0 (3)	5.5 (4)	5.9 (4)	1.1 (4)	2.9 (3)	1.3 (3)
C(16)	0.1782 (4)	0.9038 (10)	0.2133 (8)	5.5 (3)	3.7 (4)	5.3 (4)	−0.2 (4)	2.1 (3)	−0.3 (3)
C(21)	0.1500 (3)	0.8686 (8)	0.4555 (8)	3.5 (3)	2.4 (4)	4.9 (4)	−0.2 (3)	0.6 (3)	−0.4 (3)
C(22)	0.1282 (3)	0.8748 (9)	0.5296 (8)	4.5 (3)	3.7 (4)	4.1 (4)	−0.1 (3)	1.2 (3)	−0.2 (3)
C(23)	0.1386 (4)	0.7899 (11)	0.6090 (8)	6.0 (3)	4.8 (4)	4.2 (4)	−0.9 (4)	1.8 (3)	0.2 (3)
C(24)	0.1700 (4)	0.7072 (12)	0.6159 (9)	6.6 (4)	5.4 (4)	5.4 (4)	0.0 (5)	1.5 (4)	2.5 (3)
C(25)	0.1914 (4)	0.7010 (11)	0.5426 (11)	5.6 (3)	3.9 (6)	8.0 (6)	1.7 (4)	1.4 (5)	1.5 (6)
C(26)	0.1828 (3)	0.7828 (10)	0.4615 (9)	4.3 (3)	4.1 (4)	5.8 (4)	0.6 (3)	1.3 (3)	0.4 (3)
C(31)	0.0817 (3)	0.9117 (8)	0.2535 (7)	3.5 (3)	3.4 (3)	3.9 (3)	0.2 (3)	1.2 (2)	0.1 (3)
C(32)	0.0471 (3)	0.9866 (9)	0.1916 (8)	4.8 (3)	3.2 (4)	4.1 (3)	0.4 (4)	1.5 (3)	0.6 (3)
C(33)	0.0072 (3)	0.9419 (11)	0.1227 (8)	4.8 (2)	5.3 (4)	4.0 (3)	0.9 (4)	1.3 (3)	0.9 (3)
C(34)	0.0019 (3)	0.8227 (11)	0.1098 (9)	3.7 (3)	7.3 (4)	4.9 (4)	−0.3 (4)	1.3 (3)	−0.4 (6)
C(35)	0.0358 (3)	0.7520 (10)	0.1674 (9)	4.5 (3)	3.7 (4)	6.0 (4)	−0.2 (3)	1.1 (4)	−0.3 (3)
C(36)	0.0760 (3)	0.7967 (10)	0.2404 (8)	4.8 (3)	3.2 (4)	5.8 (4)	0.2 (3)	2.2 (3)	0.6 (3)

[a] The form of the anisotropic thermal parameter is $\exp[-1/4\{B_{11}(a^*h)^2 + B_{22}(b^*k)^2 + B_{33}(c^*l)^2 + 2B_{12}a^*bhk + 2B_{13}a^*c^*hl + 2B_{23}b^*c^*kl\}]$.

Table VI. Some Selected Bond Distances (Å) and Angles (Deg) for $(\eta^3\text{-}C_3H_5)Fe(CO)_3X$ with Estimated Standard Deviations

	Br	I[3]	$(\eta^3\text{-}C_3H_5)Fe(CO)_3$[4]
Fe-X	2.494 (2)	2.750 (5)	3.138 (3)
Fe-C1	2.126 (8)	2.34 (2), 2.26 (2)	2.208 (4), 2.195 (4)
Fe-C2	2.058 (11)	2.09 (2)	2.104 (4)
Fe-C4	1.791 (12)	1.79 (2)	1.837 (9)
Fe-C5	1.785 (9)	1.80 (2), 1.80 (2)	1.778 (9), 1.830 (8)
C4-O4	1.123 (12)	1.19 (3)	1.183 (8)
C5-O5	1.150 (12)	1.19 (3), 1.19 (3)	1.157 (8), 1.149 (7)
C1-C2	1.392 (10)	1.35 (3), 1.43 (3)	1.417 (5), 1.389 (5)
X-Fe-C1	88.3 (2)	99, 87	106.8 (1), 107.1 (1)
X-Fe-C2	105.2 (4)		91.6 (1)
X-Fe-C4	171.9 (4)	170	160.2 (2)
X-Fe-C5	83.5 (2)	80, 82	75.3 (3), 74.7 (2)
Fe-C4-O4	177.8 (11)	171 (1)	176.6 (8)
Fe-C5-O5	177.8 (11)	178 (1), 176 (1)	174.3 (8), 175.0 (7)
C4-Fe-C5	91.6 (3)	91.3 (9), 96.3 (9)	91.8 (4), 94.0 (3)
C5-Fe-C5′	105.9 (4)	109.3 (9)	104.8 (3)
C1-C2-C1′	124.1 (4)	131 (3)	120.4 (4)

Table VII. Some Selected Bond Distances (Å) and Angles (Deg) for $(\eta^3\text{-}C_3H_5)Fe(CO)_3AuP(C_6H_5)_3$ with Estimated Standard Deviations

Au-Fe	2.519 (1)	C1-C2	1.37 (2)
Au-P	2.273 (5)	C2-C3	1.29 (2)
Fe-C1	2.13 (1)	C4-O4	1.14 (1)
Fe-C2	1.99 (1)	C5-O5	1.14 (1)
Fe-C3	2.13 (1)	C6-O6	1.14 (1)
Fe-C4	1.773 (9)	P-C11	1.809 (7)
Fe-C5	1.773 (9)	P-C21	1.804 (7)
Fe-C6	1.789 (7)	P-C31	1.821 (6)
P-Au-Fe	174.4 (2)	C5-Fe-C6	142.9 (3)
Au-Fe-C1	97.6 (3)	C4-Fe-C6	99.1 (3)
Au-Fe-C2	134.4 (6)	C4-Fe-C5	92.5 (4)
Au-Fe-C3	163.3 (3)	Fe-C4-O4	177.0 (7)
Au-Fe-C4	106.3 (3)	Fe-C5-O5	177.4 (7)
Au-Fe-C5	72.0 (2)	Fe-C6-O6	175.3 (7)
Au-Fe-C6	70.9 (2)	C1-C2-C3	129.5 (15)

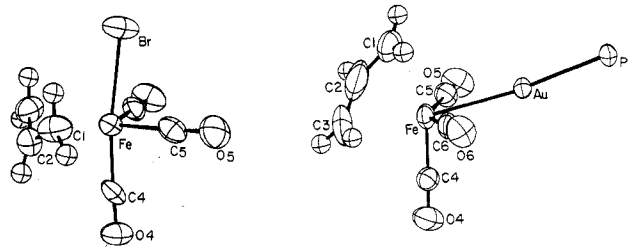

Figure 1. Approximate congruent views of $(\eta^3\text{-}C_3H_5)Fe(CO)_3Br$, I, and $(\eta^3\text{-}C_3H_5)Fe(CO)_3AuP(C_6H_5)_3$, II, showing the relative positioning of the η^3-allyl ligand. Complex I is best described as a pseudooctahedron, while II has an approximate trigonal-bipyramidal geometry with the $AuP(C_6H_5)_3$ ligand on the equatorial edge. The phenyl groups of II are not shown.

duct of the $(\eta^3\text{-}C_3H_5)Fe(CO)_3^-$ Lewis base, in accordance with Shriver's concept of transition-metal basicity.[10] The very low CO stretching frequencies observed for the gold complex are in agreement with such an assignment. The radical dimer has an Fe–Fe bond of zero polarity and represents a true intermediate case.

The NMR spectra of the halide complexes clearly show the presence of two isomers. The predominate isomer has the endo configuration. The NMR spectrum of our gold derivative contains the resonances corresponding to only one isomer and is indicative of a symmetric allyl ligand. The chemical shift values (Table II) differ considerably from those of either isomer of the halide complexes, perhaps reflecting the high negative charge on the iron atom or alternatively an indication of an entirely different molecular structure.

Structure of $(\eta^3\text{-}C_3H_5)Fe(CO)_3Br$. Since the published structure of the $(\eta^3\text{-}C_3H_5)Fe(CO)_3I$ complex[3] was a poor one (R = 15.8%) with high σ values, we determined the structure of the bromide to obtain accurate parameters of a complex

(10) Shriver, D. F. *Acc. Chem. Res.* **1970**, *3*, 231.

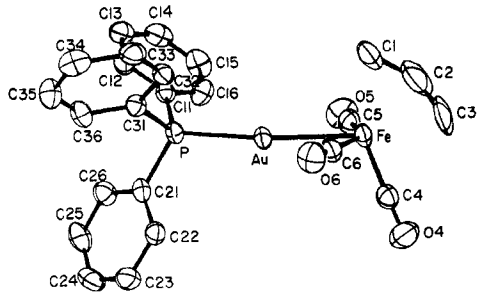

Figure 2. Perspective view of $(\eta^3\text{-}C_3H_5)Fe(CO)_3AuP(C_6H_5)_3$, II, with the crystallographic numbering scheme. Hydrogens are omitted for clarity. The atoms are represented by 33% probability ellipsoids.

with the endo geometry. The molecular structure is illustrated by Figure 1. The ligands are arranged around the iron in a pseudooctahedral geometry with some distortions caused by the geometric restrictions of the allyl ligand. The allyl ligand has the endo configuration corresponding to the predominate solution isomer.

The allyl geometry is normal with a C(1)–C(2) bond length of 1.39 (1) Å and a C(1)–C(2)–C(1)′ bond angle of 124.1 (4)°. The Fe–C(2) bond distance of 2.06 (1) Å is shorter than the distance found for the Fe–C(1) terminal bond, 2.13 (1) Å. Ibers[11] has defined allyl orientation angles as shown below, where O is the center of mass of the allyl. For this complex,

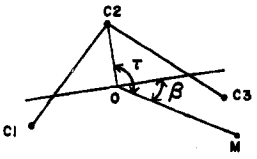

β is required to be 90.0° by symmetry and τ has a value of 117.2° which is intermediate when compared to other allyl complexes.[11] The angles between the other ligands approximate those of an octahedron. The Br–Fe–C(4) angle, 171.9 (4)°, deviates only slightly from linearity; while the largest deviation is the 105.9 (4)° angle subtended by C(5)–Fe–C(5)′.

The overall geometry of I is quite similar to that of the iodide, although the structures are not isomorphous. The geometry about the iron atom in the dimer is also similar, even though it has the exo configuration (Table VI). The X–Fe–CO angles are somewhat smaller in the dimer than in the halide derivatives, perhaps reflecting the lessened steric requirements of the more distant (3.138 (3) Å) second iron moiety.

Structure of $(\eta^3\text{-}C_3H_5)Fe(CO)_3AuP(C_6H_5)_3$. We assumed initially that the gold derivative would have either the endo or exo geometry even though the electronic structure differs significantly from the halide or pseudohalide complexes. The actual molecular geometry is most surprising and is illustrated by Figure 2. The most unusual aspect of the structure is the relative positioning of the $AuP(C_6H_5)_3^+$ substituent with respect to the CO ligands. The Au–Fe bond bisects the C(5)–Fe–C(6) angle (142.9 (3)°) resulting in a planar unit containing the two metal atoms and the two carbonyl ligands. The Au–Fe–C(5);C(6) angles are 72.0 (2)° and 70.9 (2)° with Au–C(5);C(6) distances of 2.595 (7) and 2.569 (7) Å, respectively. The Au–Fe bond distance of 2.519 (1) Å is equal to the sum of the Pauling metallic radii[12] (Fe = 1.17 Å; Au = 1.34 Å).

Figure 1 shows approximate congruent views of the bromide and gold derivatives. Not only has the gold atom moved between the two equatorial CO ligands but also the allyl has rotated 90° and has an orientation intermediate with respect to both endo and exo configurations. The allyl bond parameters are not unusual, with C(1)–C(2) and C(2)–C(3) distances of 1.37 (2) and 1.29 (2) Å, respectively, and the C(1)–C(2)–C(3) angle of 129 (1)°. The τ and β angles are 111.0° and 88.7°, respectively.

The best description of the unusual structure may be as a distorted trigonal-bipyramidal $(\eta^3\text{-}C_3H_5)Fe(CO)_3^-$ anion with a $AuP(C_6H_5)_3^+$ cation on an equatorial edge.[13] The bidentate allyl ligand spans an equatorial and an axial site, with the three carbonyl ligands occupying the remaining sites. The C(5)–Fe–C(6) angle is opened up from the ideal 120° to 142.9 (3)° to accommodate the edge-bound gold atom. The coordination about the gold atom is linear as expected for gold(I) complexes with a normal Au–P bond distance of 2.273 (5) Å.

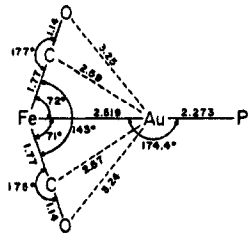

The NMR spectrum of the gold derivative, II, indicates that there is only one species in solution and that the two ends of the allyl are equivalent over the NMR time scale. The structure found in the crystalline state is not compatible with this solution result. Either the solution structure is simply different, perhaps corresponding to either of the conventional endo or exo allyl orientations, or there is a dynamic process of allyl rotation in solution which equilibrates the two ends of the allyl. To test the latter possibility, we cooled an acetone solution of the complex to −90 °C but saw no significant changes in the NMR spectrum. This does not rule out a dynamic process, however, since many low-energy pathways can be envisioned. We prepared the cinnamyl analogue, IV, in order to impose asymmetry on the allyl ligand and again found NMR evidence for only one isomer. The NMR results were not as conclusive in this case since the compound proved to be rather unstable and paramagnetic impurities formed rapidly.

Bonding Description. The unusual arrangement of the carbonyl ligands in the gold derivative is similar to the geometry found in other compounds which are said to contain semibridging carbonyl ligands.[14] The existence of semibridging carbonyls in compounds with polar metal–metal bonds has been discussed by Cotton[15] who hypothesized that the primary interaction between the more distant second metal atom and the semibridged carbonyl ligand was due to a donation of electron density into the CO π^* orbitals. This description does not seem applicable to the gold derivatives since the 14-electron gold(I) center is not a very good π-electron donor.[16] Others have proposed that semibridging carbonyls are controlled by sterics alone,[17] but in the molecules con-

(11) Kaduk, J. A.; Poulos, A. T.; Ibers, J. A. *J. Organomet. Chem.* **1977**, *127*, 245.
(12) Pauling, L. In "The Nature of the Chemical Bond", 3rd ed.; Cornell University Press: Ithaca, N.Y., 1960; p 104.
(13) Examples of edge-bridged $Co(CO)^{4-}$ anions are known: (a) LeBorgne, G.; Bouaoud, S.; Grandjean, D.; Braunstein, P.; DeHand, J.; Pfeffer, M. *J. Organomet. Chem.* **1970**, *136*, 375. (b) Chin, H. B.; Smith, M. B.; Wilson, R. D.; Bau, R. *J. Am. Chem. Soc.* **1974**, *96*, 5285.
(14) (a) Cotton, F. A.; Kruczynski, L.; Frenz, B. A. *J. Organomet. Chem.* **1978**, *160*, 93. (b) McNeill, E. A.; Scholer, F. R. *J. Am. Chem. Soc.* **1977**, *99*, 6243. (c) St. Denis, J.; Butler, W.; Glick, M. D.; Oliver, J. P. *Ibid.* **1974**, *96*, 5427.
(15) (a) Cotton, F. A.; Troup, J. M. *J. Am. Chem. Soc.* **1974**, *96*, 1233. (b) Cotton, F. A. *Prog. Inorg. Chem.*, **1976**, *21*, 1. (c) Bailey, W. I.; Collins, D. M.; Cotton, F. A. *J. Organomet. Chem.* **1977**, *135*, C53.
(16) (a) Graham, W. A. G. *Inorg. Chem.* **1968**, *7*, 315. (b) Johnson, B. F. G.; Davis, R. In "Comprehensive Inorganic Chemistry"; Bailar, J. C., Ed.; Pergamon Press: Oxford, 1973; Vol. 3, Chapter 3.
(17) Colton, R.; McCormick, M. J. *Coord. Chem. Rev.* **1980**, *31*, 1.

sidered here the steric constraints within the gold complex are essentially identical with those of the bromide. An alternative electronic explanation for the quite angular arrangement has been developed on the basis of a molecular orbital study of transition-metal basicity which we plan to publish elsewhere. We believe that the observed structure is a consequence of the reverse polarity of the iron–gold bond. The $(\eta^3\text{-}C_3H_5)Fe(CO)_3^-$ anion is acting as a Lewis base and the $AuP(C_6H_5)_3^+$ cation as the Lewis acid. The electrons of the resulting donor–acceptor bond are located primarily on the iron atom and are primarily of d character. Since d orbitals have a multinodal structure they show little stereochemical activity when compared to orbitals with high s and p character. Since the electrons of the Fe–Au bond are not stereochemically active, the angles to the neighboring CO ligands are acute. The low angles are thus a direct consequence of the transition-metal basicity and do not reflect any direct interaction between the gold atom and the CO ligands. In the bromide derivative, I, the electrons of the Fe–Br bond are located primarily on the Br^- donor atom, while the acceptor orbital on the Fe moiety is of high s and p character and is thus stereochemically active.

The concept that the effective hybridization of a central atom, and thus its geometry, is dependent upon the nature of the substituents is certainly not a new one and many standard textbook examples are known in main-group chemistry. This concept, however, has not been routinely applied to transition-metal complexes. We believe the effect of the substituents is particularly important in molecules with polar metal–metal bonds as well as in other metal–Lewis acid adducts in which acute angles to cis ligands are found. The assignment of geometry has been most often discussed in terms of the stereochemical activity of the hydride ligand;[19] but the stereochemical consequences of polar bonds between two different metals are often even more dramatic. For example,[20] in the C_{3v} molecule $Co(CO)_4H$, the average angle between the hydride and the three cis CO ligands is 80°, which is far from the ideal value of 90°. In the analogous gold complex[21] $Co(CO)_4AuP(C_6H_5)_3$ the cis angles are only 77°.

In summary, we propose that the distinctly different coordination geometries of the gold and bromide complexes are directly due to the reversed polarity of the iron–gold bond as compared to the iron–bromide bond. We believe that this phenomenon can be observed in a wide range of compounds and that it deserves further investigation.

Registry No. I, 12192-46-0; II, 73891-25-5; III, 12288-77-6; IV, 73891-24-4; $AuPPh_3Cl$, 14243-64-2.

Supplementary Material Available: Listings of structure factor amplitudes and positional and thermal parameters for the hydrogens of $(\eta^3\text{-}C_3H_5)Fe(CO)_3Br$ and $(\eta^3\text{-}C_3H_5)Fe(CO)_3AuP(C_6H_5)_3$ (16 pages). Ordering information is given on any current masthead page.

(18) Simon, F. E.; Lauher, J. W., manuscript in preparation.

(19) Frenz, B. A.; Ibers, J. A. In "Transition Metal Hydrides"; Meutterties, E. L., Ed.; Marcel Dekker: New York, 1971; Vol. 1, Chapter 3.
(20) McNeill, E. A.; Scholer, F. R. *J. Am. Chem. Soc.* **1977**, *99*, 6243.
(21) Blundell, T. L.; Powell, H. M. *J. Chem. Soc. A* **1971**, 1685.

Contribution from the Departments of Chemistry and Physics and Astronomy, Vanderbilt University, Nashville, Tennessee 37235

Reactions of Coordinated Molecules. 26. Crystal and Molecular Structure of $[\eta^5\text{-}C_5H_5(OC)Fe(CH_3CO)(i\text{-}C_3H_7CO)]BF_2$: A Metalla-β-diketonate Complex of Boron

P. GALEN LENHERT,*[1a] C. M. LUKEHART,*[1b,c] and L. T. WARFIELD[1b]

Received December 5, 1979

The complex $[\eta^5\text{-}C_5H_5(OC)Fe(CH_3CO)(i\text{-}C_3H_7CO)]BF_2$ crystallizes in the monoclinic space group $P2_1/c$ with a = 8.0972 (11) Å, b = 11.548 (2) Å, c = 15.393 (3) Å, β = 111.77 (1)°, V = 1337 Å^3, Z = 4, and ρ(calcd) = 1.550 g cm^{-3} for mol wt 311.92. Diffraction data (2θ out to 60°) were collected with a four-circle diffractometer using Nb-filtered Mo Kα radiation. The structure was refined by using the full-matrix least-squares procedure, and the resulting discrepancy indices were R = 4.8% and R_w = 3.3% for 3891 independent reflections. The boron atom acts as the central coordinating atom with the BF_2 moiety being bonded to the ferra-β-diketonate ligand through the two oxygen atoms of the metallachelate ring. The atoms comprising the backbone of the metallachelate ring are not coplanar, and the chelate ring adopts a boat-shaped structure. This complex is the second example of a nonplanar, metalla-β-diketonate ring structure, and this nonplanar ring conformation is attributed to the relief of internal angle strain within the metallachelate ring due to the bonding preferences imposed by the metalla and the central coordinating atoms.

Introduction

The discovery of the metalla-β-diketonate molecules initiated a study of the coordination chemistry and the organic condensation chemistry of these complexes. The elucidation of the molecular structures of these metalla molecules is an important aspect of this continuing investigation.

The structures of three metallaacetylacetonate complexes, **1**–**3**, have been determined previously by X-ray crystallography.[2-4] Complex **1** is the neutral tris(metallaacetylacetonate) complex of Al(III) where the metalla moiety is the *cis*-$Mn(CO)_4$ group, and the complexes **2** and **3** are neutral metallaacetylacetonate molecules where the metalla moiety is the analogous rhenium fragment. In **1** and **2** the metallaacetyl-

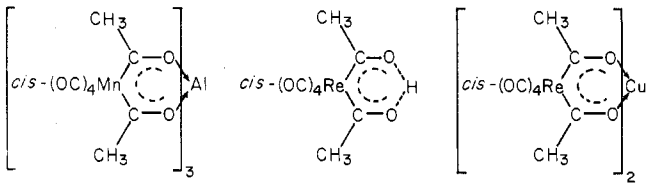

1 **2** **3**

(1) (a) Department of Physics and Astronomy. (b) Department of Chemistry. (c) Research Fellow of the Alfred P. Sloan Foundation (1979–1981).
(2) Lukehart, C. M.; Torrence, G. P.; Zeile, J. V. *J. Am. Chem. Soc.* **1975**, *97*, 6903.
(3) Lukehart, C. M.; Zeile, J. V. *J. Am. Chem. Soc.* **1976**, *98*, 2365.
(4) Lenhert, P. G.; Lukehart, C. M.; Warfield, L. T. *Inorg. Chem.* **1980**, *19*, 311.

0020-1669/80/1319-2343$01.00/0